THE JOURNAL OF BIOLOGICAL CHEMISTRY
Vol. 279, No. 5, Issue of January 30, pp. 3318–3326, 2004
Printed in U.S.A.

Determination of Transmembrane Topology of the *Escherichia coli* Natural Resistance-associated Macrophage Protein (Nramp) Ortholog*[S]

Received for publication, September 8, 2003, and in revised form, November 6, 2003
Published, JBC Papers in Press, November 7, 2003, DOI 10.1074/jbc.M309913200

Pascal Courville‡, Roman Chaloupka‡§¶, Frédéric Veyrier‡, and Mathieu F. M. Cellier‡‖

From the ‡Institut National de la Recherche Scientifique-Institut Armand-Frappier, Laval, Québec, Canada H7V 1B7 and the §Institute of Physics, Charles University in Prague, Ke Karlovu 5, 121 16 Prague 2, Czech Republic

The natural resistance-associated macrophage protein (Nramp) defines a conserved family of secondary metal transporters. Molecular evolutionary analysis of the Nramp family revealed the early duplication of an ancestral eukaryotic *Nramp* gene, which was likely derived from a bacterial ortholog and characterized as a proton-dependent manganese transporter MntH (Makui, H., Roig, E., Cole, S. T., Helmann, J. D., Gros, P., and Cellier, M. F. (2000) *Mol. Microbiol.* 35, 1065–1078). *Escherichia coli* MntH represents a model of choice to study structure function relationship in the Nramp protein family. Here, we report *E. coli* MntH transmembrane topology using a combination of *in silico* predictions, genetic fusion with cytoplasmic and periplasmic reporters, and MntH functional assays. Constructs of the secreted form of β-lactamase (Blam) revealed extra loops between transmembrane domains 1/2, 5/6, 7/8, and 9/10, and placed the C terminus periplasmically; chloramphenicol acetyltransferase constructs indicated cytoplasmic loops 2/3, 6/7, 8/9, and 10/11. Two intra loops for which no data were produced (N terminus, intra loop 4/5) both display composition bias supporting their deduced localization. The extra loops 5/6 and 6/7 and periplasmic exposure of the C terminus were confirmed by targeted reporter insertion. Three of them preserved MntH function as measured by a disk assay of divalent metal uptake and a fluorescence assay of divalent metal-dependent proton transport, whereas a truncated form lacking transmembrane domain 11 was inactive. These results demonstrate that EcoliA is a type III integral membrane protein with 11 transmembrane domains transporting both divalent metal ions and protons.

Divalent metal ions such as ferrous iron, Fe^{2+}, Mn^{2+}, Co^{2+}, and Zn^{2+} are vital nutrients for living cells that participate as metabolic cofactors in a variety of biochemical processes involving electron transfers, including respiration and photosynthesis. The natural resistance-associated macrophage protein (Nramp)[1] belongs to a highly conserved family of integral membrane proteins found in a large spectrum of organisms, including mammals (2, 3), plants (4), yeast (5), and bacteria (6, 7). Eukaryotic Nramp proteins were implicated in pH-dependent transport of divalent metals, including Fe^{2+} and Mn^{2+} (8, 9). Mammalian Nramp2 facilitates transferrin-independent iron absorption in the intestine and transferrin-dependent iron uptake by peripheral tissues (*e.g.* bone marrow, erythrocytes, and kidney), whereas Nramp1 is devoted to host resistance, acting at the level of the membrane of the phagosome in macrophages and neutrophils (10). Likewise, three yeast homologs contribute to manganese and iron homeostasis by facilitating manganese acquisition either at the plasma membrane or from intracellular vesicles and iron mobilization from the vacuole (11). The phenotypes associated with *Nramp1* and *Nramp2* knockout in mice, innate susceptibility to various intracellular pathogens and microcytic anemia, respectively, demonstrate nonredundant roles of mammalian Nramp proteins in divalent metal homeostasis. Deregulation of their expression may also perturb normal metabolism due to the cytotoxic effects of excessive metal accumulation (12).

Bacterial homologs of eukaryotic Nramp were subsequently characterized in Gram-positive and -negative species as proton-dependent manganese transporters and denominated MntH proteins. Detailed sequence analyses revealed the existence of three phylogenetic groups of MntH proteins that showed distinct evolutionary patterns, and these groups were designated MntH A, B, and C (13). One of three phylogenetic groups of bacterial homologs (1) is distributed among Gram-positive and -negative bacteria and shows congruency between function, phylogenetic and taxonomic relationships, and amino acid substitution rate pattern, consistent with an early evolutionary origin (14). Several MntH A proteins were functionally characterized. In Gram-positive species, *Bacillus subtilis* MntH A is necessary for growth in minimal medium not supplemented with manganese, and *mntH* gene expression is regulated by the manganese-dependent repressor MntR (15). Mycobacterial MntH A was characterized by heterologous expression in *Xenopus* oocytes (16) and yeast (17). MntH A proteins were also studied in Gram-negative species; *Escherichia coli* and *Salmonella typhimurium* MntH A proteins were characterized in our laboratory as proton-dependent transporters of divalent metals with strong preference for Mn^{2+} (1, 18). MntH proteins B and

* This work was supported by Canadian Institutes of Health Research Grant MOP-78014-MI. The costs of publication of this article were defrayed in part by the payment of page charges. This article must therefore be hereby marked "*advertisement*" in accordance with 18 U.S.C. Section 1734 solely to indicate this fact.

[S] The on-line version of this article (available at http://www.jbc.org) contains a table and graph depicting impairment of EcoliA transport activity (Supplemental Data 1) and expression of Cat fusion proteins shown by SDS-PAGE (Supplemental Data 2).

¶ Supported by short term NATO Science Fellowship Grant CZ 3/2003.

‖ Scholar of the Fond pour la Recherche en Santé du Québec and to whom correspondence should be addressed: INRS-Institut Armand-Frappier, 531, Bd. des Prairies, Laval, Québec, Canada H7V 1B7. Tel.: 450-687-5010 (ext. 4681); Fax: 450-686-5301; E-mail: mathieu.cellier@inrs-iaf.uquebec.ca.

[1] The abbreviations used are: Nramp, natural resistance-associated protein; Blam, β-lactamase (secreted form); Cat, chloramphenicol acetyl transferase; LB, Luria-Bertani; PBS, phosphate-buffered saline; TMD, transmembrane domain; MntH, proton-dependent manganese transporter.

TABLE I
Sequence of the oligonucleotide primers used in this study

Primer	Sequence[a,b]	Restriction site
NcoI25	5′ TCACCATGGCGAACTATCGC-3′	NcoI
XbaIR	5′-AGGTCGACTCTAGAGGA-3′	XbaI
BlaM-179	5′-AACCTGGGATCCGCGCAGCTG-3′	BamHI
BlaM-263	5′-ACTTTGGATCCTCCGGTCATACT-3′	BamHI
Cat91Δ	5′-ACTACAGATCTACGCGGATAGT-3′	BglII
Cat226	5′-ATGGCGGATCCGGTTCGCGTC-3′	BamHI
Cat373	5′-TCAACTTGCTGAATCCGTCG-3′	BamHI
Cat226Δ	5′-CGCGTCTAGAATCCAAACTGC-3′	XbaI
Cat373Δ	5′-AACTTCTAGAATCCAAACTGCA-3′	XbaI
Cat324Δ	5′-GCACAGATCTCAGCGGGATAT-3′	BglII
Cat387Δ	5′-CA GCC AGA TCT TTT TAC GCG TTT-3′	BglII
PCTAG1	5′-CCACCAAATGGGATGTGGCTATC-3′	XcmI
PCTAG2	5′ ATTGGATCCCAATCCCAGCGCCGTCCCC-3′	BamHI
PCTAG3a	5′ CGCTGGGATCCTAGTTGAATGAGCGTC-3′	BamHI
PCTAG4a	5′ GCCCGAGGCATAGACTGTACAAA-3′	BsrGI
FT1	5′ ACTCTAGA*TCAGATCCTCTTCTGAGATGAGTTTTTGTTC*CAATCCCAGCGCCGTCCCCA-3′	XbaI
FT2	5′-TTGCCGCGGCTTACATTGTCGAGT-3′	SacII
Bla1	5′-CTCGTGCACCCAACTGA-3′	
BamBla1	5′ GTTGGATCCCACCCAGAAACGCTGGTGAAA-3′	BamHI
BamBla2	5′ TGAGGATCCCCAATGCTTAATCAGTGAGGCAC-3′	BamHI
CatF	5′ GCTAAGGGATCCAGCCTGCAGAAAAAAATCACTG-3′	BamHI
CatR	5′ ACTGGATCCAAACTGCAGCGCCAGCGCCCCGCCCTGCC-3′	BamHI

[a] The underlined sequences represent the localization of the restriction site.
[b] The italicized sequences represent the c-Myc tag epitope.

C have also been studied recently; one MntH C protein was reported to contribute to *Staphylococcus aureus* virulence (19), and several *mntH* genes from groups B and C were functionally expressed in *E. coli* and shown to confer sensitivity to divalent metals (14). Therefore, despite significant distance between currently known Nramp homologs, their sequence preserved structural features that correspond to a conserved function in proton-dependent divalent metal uptake.

Based on their evolutionary features, the prokaryotic genes of *mntH* group A most likely represent precursors of eukaryotic *Nramp* genes (13, 14); the corresponding proteins should thus exhibit similar structures because they perform similar functions (20). Determination of the transmembrane topology is a prerequisite to study the structural and functional properties of a membrane transporter (21), and a combination of *in silico* predictions and experimental validation is desirable to establish a reliable topological model (22). Initially, in the absence of a functional hint, extensive sequence analysis of eukaryotic Nramp homologs yielded a consensus transmembrane topology that was based on several conserved features as follows: (i) the presence of ten hydrophobic segments showing a remarkable degree of amino acid sequence conservation, including, for some, the presence of charged residues and overall amphiphilic character; (ii) the strong net positive charge for hydrophilic loops predicted to be cytoplasmic; and (iii) the presence of a potential glycosylation signal in a predicted extracytoplasmic loop and a putative conserved transport motif. This putative topology placed the N terminus cytoplasmically followed by a conserved hydrophobic core of ten transmembrane domains (TMD) and either one or two non-conserved, highly hydrophobic TMDs (placing the C terminus extra- or intra-cytoplasmically, respectively).

The proposed topology has been verified in different regions of different homologs. The orientation of yeast Smf3p TMD11 has been determined by inserting a hemagglutinin A tag at either end of this segment. Only the C-terminal insertion was removed by vacuolar proteases consistent with the location of Smf3p in the membrane of the yeast vacuole. The data indicated that the last TMD in yeast Smf proteins is oriented from the cytoplasm toward the exterior, placing the C terminus extracytoplasmically (11). Both the N and C termini of the mammalian protein Nramp1 were localized on the cytoplasmic side of the membrane using either a polyclonal serum generated against the N-terminal portion of the protein or by creating a c-Myc tag insertion at the C terminus (23). The same group found, using the paralogous Nramp2, that the loop between the TMDs 7 and 8 was extracellular after inserting a hemagglutinin A tag (24). Recently, a study indicated that a 24-residue peptide corresponding to Nramp2 putative TMD4 (residues 179–202) adopted a well folded α-helical conformation from the residue Val^{187} to Lys^{201} in detergent micelles (25).

Alternative topologies have been proposed; one study suggested that mouse Nramp1 could adopt a reverse transmembrane topology (extracytoplasmic N and C termini) based on findings that incubation with antibodies directed against either the predicted extra loop between TMDs 7 and 8 or the C terminus inhibited or did not inhibit, respectively, temperature-dependent association of iron with purified phagosomes (26). Concerning bacterial homologs, a study of the reactivity of the unique cysteine of the *Mycobacterium leprae* MntH A protein proposed a transmembrane topology inferred from sequence-based predictions that included 12 TMDs (17). These data raise the issue of the number of TMDs in prokaryotic MntH proteins and of the similarity of prokaryotic MntH and eukaryotic Nramp and Smfp transmembrane organization.

In the present study, we investigated the transmembrane topology of the *E. coli* Nramp ortholog MntH A (EcoliA), which constitutes an ideal structural and functional model of eukaryotic Nramp using different genetic approaches. We employed a combination of *in silico* predictions, reporter gene fusions, and insertion mutagenesis, including bi-functional hybrid proteins for which metal uptake and metal-dependent proton transport were evaluated.

EXPERIMENTAL PROCEDURES

Bacterial Strains and Growth Conditions—DH11S *mntH E. coli* cells (kanamycin-resistant) were used in the standard cloning procedures. Bacteria were grown at 37 °C and 250 rpm in Luria-Bertani (LB) broth supplemented with the appropriated antibiotics (100 μg/ml ampicillin, 30 μg/ml kanamycin, or 15 μg/ml gentamicin). The GTA medium (1) was used for the disc assay and complementation experiment using the SL93 *mntH E. coli* strain (Tables I and II).

Sequence Analyses—Three programs were used to formulate a consensus prediction topology of the MntH A protein, namely TMHMM

TABLE II
Bacterial strains and plasmids used in this study

The abbreviations used include the following: Amp^r, ampicillin-resistant; Gm^r, gentamicin-resistant; IPTG, isopropyl-1-thio-β -D-galactopyranoside; Kan^r, kanamycin-resistant; Tc^r, tetracyclin-resistant.

Strains and plasmids	Genotype or other relevant characteristics	Reference or source
DH11S	F$^-$ *mcr*A Δ (*mrr hsd*RMS *mcr*BC) Δ (*lac-pro*AB) Δ (*rec*A1398) *deo*R *sup*E *rps*L *srl thi*/F′ *pro*AB$^+$*lac*I^{q}Z ΔM15	Invitrogen
SL93	*lac-3350*, *galK2*, *galT22*, *rpsL179*, zgj-203::Tn10 *hflB1* (Ts)	53
SL93 *mntH*		1
pBADNX1.1[a]	Amp^r and induction with L-arabinose	1
pBADNX7.2[b]	Gm^r and induction with L-arabinose	This study
pBADGmΔBamHI	Gm^r and not inducible	This study
pYZ4NX1.1	Kan^r and induction with IPTG	This study
pYZ5	Tc^r Blam fusion vector	27

[a] This plasmid was used for most cloning experiments.
[b] This plasmid was used to clone the Blam insertions.

(www.cbs.dtu.dk/services/TMHMM-2.0/), PHDhtm (cubic.bioc.columbia.edu/predictprotein/), and MEMSAT (bioinf.cs.ucl.ac.uk/psiform.html). Hydrophobicity profiles were generated using the method of Kyte and Doolittle (Ref. 42; for an example, see www.bio.davidson.edu/courses/compbio/flc/home.html) and by implementing a sliding window of 19 residues.

Construction and Analysis of Random β-Lactamase (Blam) Fusions—pBAD NX1.1 was subcloned in pYZ4 (28). Nested 3′ deletions of the *mntH* gene were obtained by digesting pYZ4 NX1.1 with XbaI and SphI and treated with exonuclease III using the Exo-size™ deletion kit (New England Biolabs, Mississauga, Ontario, Canada) according to the manufacturer's instructions. The fusion at the amino acid Ala^{165} was obtained by digesting pYZ4 NX1.1 with SacII and treating with T4 DNA polymerase to create blunt ends conserving the reading frame. The different preparations were digested with SacI, purified, and ligated with the 850-bp secreted Blam open reading frame, previously obtained by digestion with PvuII and SacI of the plasmid pYZ5 (27). The ligation product was transformed in *E. coli* competent cell DH11S, and kanamycin-resistant transformants were selected. The colonies were scratched on three plates containing, respectively, 30 μg/ml kanamycin and 20 and 100 μg/ml ampicillin. All plates contained 10 μM isopropyl β-D-1-thiogalactopyranoside, and ampicillin-resistant and kanamycin-resistant colonies were selected. The minimal inhibitory concentration of ampicillin for the MntH-Blam fusions were determined by spotting 4 μl of a diluted 16-h liquid culture (10^{-5} and 10^{-6}) on plates containing different concentrations of ampicillin and supplemented with isopropyl β-D-1-thiogalactopyranoside. Plasmids were isolated from selected clones (>45 μg/ml ampicillin) and analyzed with restriction enzymes to determine the approximate position of the fusion. Those corresponding to novel positions were sequenced using automatic sequencer CEQ 2000XL from Beckman Coulter (Mississauga, Ontario, Canada).

Construction and Analysis of Targeted Chloramphenicol Acetyltransferase (Cat) Fusions—Cat constructions were created by targeted PCR fusion inserting BglII sites after the amino acids Leu^{324} and Lys^{387}. The products were digested with SacII and BglII and ligated to the vector pBADNX1.1 digested with the SacII and XbaI and to the *cat* gene amplified by PCR and containing 5′-BamHI and a 3′-XbaI sites. The fusions at the residues Gly^{226} and Leu^{412} were constructed using NcoI and BamHI sites, and a BglII site was used at Arg^{91}. The different fusions were tested for resistance to chloramphenicol using a 16-h liquid culture to inoculate 2 ml of LB medium (1/10) and grown for 3 h under agitation. Cultures were then induced to express the constructs with 0.06% L-arabinose for 1 h, and 4 μl of a 10^4 dilution were spotted on plates containing different chloramphenicol concentrations and 0.2% L-arabinose (except for the construct L^{412}-Cat, for which 6×10^{-5} % L-arabinose was used). Constructs Thr^{371} and Leu^{404} were subcloned in pBADNX1.1 and pBADNX7.1, respectively, using NcoI and SphI restriction sites.

Construction and Analysis of Targeted Insertions—Targeted Blam insertions were obtained by PCR overlap extension to introduce BamHI sites (29) after the amino acids Leu^{179}, Phe^{263}, and Leu^{412}. The final products were cloned in pBADGmΔBamHI using NcoI and XbaI restriction sites. The mutants were digested with BamHI and ligated to a BamHI Blam open reading frame. The hybrid proteins were subcloned in pBADNX7.1, and ampicillin minimal inhibitory concentrations were obtained as described above using a subtoxic concentration of L-arabinose as an inducer of expression. The PCR overlap extension approach was also used to generate a C-terminal c-Myc fusion (EQKLISEEDL). The toxicity of the constructs was estimated by growing a LB culture for 16 h at 37 °C and 250 rpm, which was then diluted in fresh LB broth to obtain a final optical density (OD_{600}) of 0.5 and subcultured in the presence of different concentrations of L-arabinose during a 6-h period. The level of toxicity of the mutants was estimated from the final OD_{600}.

Western Blot Analysis—Cytoplasmic and membrane fractions were prepared for each random fusion (30). The samples were solubilized in SDS dissolving buffer (4% (w/v) SDS, 40% (v/v) glycerol, 0.5 M mercaptoethanol, 40 mM Tris-HCl, pH7.2, and 0.005% (w/v) bromphenol blue) and incubated at 37 °C for 30 min. Proteins were separated by electrophoresis using a 12% polyacrylamide gel (SDS-PAGE). The proteins were transferred on a sequi-blot polyvinylidene fluoride membrane from Bio-Rad at 60 mA for 1 h, washed with distilled H_2O, and blocked for 16 h at 4 °C in a 1× 0.1% PBS-Tween 20 solution containing 5% milk. Membrane were incubated with the primary antibody for 1 h, washed four times for 12 min in 0.1% PBS-Tween 20, and incubated for 1 h with the secondary antibody (anti-IgG1-horseradish peroxidase (Santa Cruz Biotechnology, Santa Cruz, CA; 1:1000) and four 12-min washes in 0.1% PBS-Tween 20. Blots were revealed using the ECL Western blotting reagent from Amersham Biosciences. The primary antibodies used were an anti-β-lactamase monoclonal antibody (Biodesign International, Saco, ME; 1:500), an anti-c-Myc monoclonal (antibody Biodesign International; 1:100), and anti-Cat polyclonal antibody (Sigma; 1:700).

Protein Overexpression and Preparation of Mixed Membranes—Membrane extracts were obtained by the preparation of *E. coli* mixed membranes using a water lysis protocol (31). In brief, 50 ml of *E. coli* culture induced for 16 h with 0.06% of L-arabinose were harvested and lysed in sucrose buffer containing EDTA and lysozyme. The spheroplasts were harvested and incubated for 30 min in deionized water. The mixed membranes were then washed and resuspended in 400 μl of membrane resuspension buffer (0.1 M sodium phosphate, pH 7.2, and 1 mM 2-mercaptoethanol). 120 μg of total proteins were separated on SDS-PAGE, and Western blot was performed as described above. Protein concentrations were determined using the non-interfering protein assay by Genotech (St. Louis, MO).

MntH A Functional Assays—MntH-dependent metal uptake was evaluated by a disk assay of metal sensitivity. Cells were grown during a 16-h period at 37 °C and 250 rpm. The cultures were then diluted in the GTA broth to obtain a final OD_{600} of 0.55. 100 μl of bacteria was mixed to 3 ml of molted GTA agar and spread onto GTA plates supplemented with the appropriate concentration of arabinose prior to placing a disk impregnated with 10 μl of metallic solution and incubating for 16 h at 37 or 42 °C (1). MntH- and divalent metal-dependent intracellular accumulation of protons was determined by measuring the fluorescence intensity ratio of pH-dependent ratiometric GFP (pHluorin) (32, 33).

Electro-competent cells of *E. coli* DH11S *mntH* were transformed with pGBM6-pH constructed as follows. pHluorin (GenBank™ accession AF058694) was amplified by PCR from pGFPratiometric (32) using the primers Gratio2F (5′-AAAAGCATGCGTAAAGGAGAAGAACT-3′) and Gratio2R (5′-TATTAAGCTTTTATTTGTATAGTTCATCC-3′). Cycling parameters with the *Pfu* polymerase (Stratagene, Cedar Creek, TX), were 5 cycles of 96 °C for 45 s, 55 °C for 45 s, and 72 °C for 2 min 30 s, followed by 25 cycles of 96 °C for 45 s, 62 °C for 45 s, and 72 °C for 2 min 30 s. This fragment was cloned into pJBA111 (34) using SphI and HindIII restrictions sites. Subsequently, the cassette $P_{A1/04/03}$-RBSII-gfp ratio-T0-T1, was excised using NotI, blunt-ended using T4 DNA polymerase, and ligated to pGBM6 (ATCC 87502), which was digested previously by SmaI.

For transport activity determination, TSS-competent cells of *E. coli* DH11S *mntH* (pGBM6-pH) were transformed with pBAD plasmids

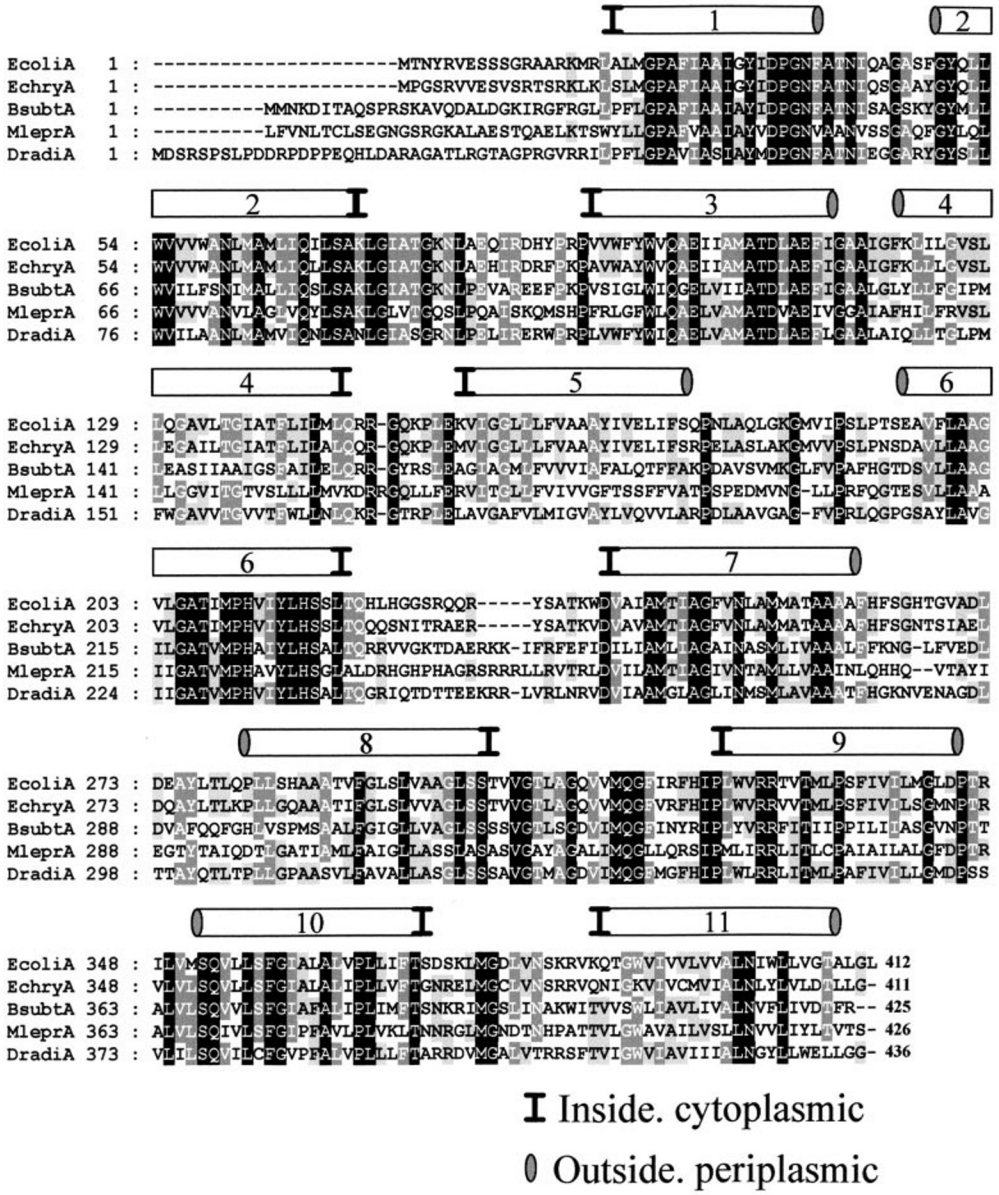

FIG. 1. **Sequence analysis of selected MntH homologs from group A.** The *open boxes* above the alignment indicate putative transmembrane segments, and their orientation relative to the membrane as predicted by different algorithms. The homologs and the species from which they were derived are: EcoliA, *E. coli*; EchryA, *Erwinia chrysanthemi*; BsubtA, *B. subtilis*; MleprA, *M. leprae*; and DradiA, *Deinococcus radiodurans*.

encoding different MntH variants. Clones were grown in the presence of appropriate antibiotics at 37 °C in LB broth, which was supplemented with 0.06% L-arabinose 1 h before fluorescence measurement to allow the expression of MntH proteins. Cells were then harvested by centrifugation, washed once in citrate-potassium phosphate buffer (50 mM, pH 5), and finally resuspended in the same buffer to an OD_{600} of 0.2.

Fluorescence was measured on a Cary Eclipse fluorescence spectrophotometer (VARIAN, Inc.); pHluorin fluorescence was excited by a xenon lamp at 410 and 470 nm respectively, the emission was detected at 520 nm. Fluorescence excitation ratio *R* (410/470 nm) was continuously monitored for 500 s and transformed into pH values (or intracellular concentration of protons) according to the calibration curve. Calibration was performed by the use of carbonyl cyanide-*m*-chlorophenylhydrazone as described previously (32). Cadmium (10 μM or 100 μM) or magnesium (100 μM) were added to the samples 80 s after the beginning of the acquisition.

RESULTS

A consensus topology prediction (35) was generated to verify whether prokaryotic MntH could assume a transmembrane organization similar to eukaryotic Nramp. Algorithms using different approaches that performed best in test predictions (36–38) were employed. Memsat is a dynamic program using statistical amino acid distribution derived from well characterized membrane proteins and five structural states (inside loop, inside helix end, helix middle, outside helix end, and outside loop), to recognize possible topology models and produce a list of all possible topologies and number of TMDs (39). TMHMM uses hidden Markov simulations that implement a model defined by seven structural classes of residues constituting a membrane protein (40). To increase the accuracy of our prediction, we performed a PHDhtm transmembrane topology prediction using the evolutionary information (41) contained in a representative set of MntH A proteins from Gram-positive and -negative species and the *Deinococcus* group. In addition, an *E. coli* MntH A (EcoliA) hydropathy profile was inspected using the amino acid hydrophobicity scale of Kyte and Doolittle and a sliding window of 19 residues that discriminates best potential transmembrane helices (42). The combined results of these approaches were very consistent with those obtained with eukaryotic Nramp sequences (7) and yielded a predicted topology

TABLE III
Characterization of EcoliA Blam constructs

The abbreviations used include the following: A, ambiguous; Amp^R, ampicillin resistance; NA, not applicable; NT, not tested; P, periplasmic; RF, random fusion; TF, targeted fusion; TI, targeted insertion; TM, transmembrane.

Blam fusion point	Methods	Amp^R	Sensitivity to Manganese (1)	Suppress *HflB1* (Ts) defect	Location
		μg/ml			
Phe^{38}	RF	>300	NT	NT	P
Gly^{49}	RF	>300	NT	NT	P
Ala^{165}	TF	45	NT	NT	TM
Leu^{179}	TI	>300	−	−	P
Phe^{248}	RF	>300	NT	NT	P
Phe^{263}	TI	>300	−	+	P
Val^{350}	RF	>300	NT	NT	P
Thr^{371}	RF	100	NT	−	A
Met^{377}	RF	200	NT	NT	A
Gly^{378}	RF	200	NT	NT	A
Leu^{404}	RF	>300	−	+/−	P
Leu^{412}	TI	>300	+	++	P
EcoliA	NA	NA	++	+++	NA
Leu^{412}-c-Myc	TI	NA	+	++	NT

with the N terminus cytoplasmic, followed by 11 TMDs and the C terminus extracytoplasmic (Fig. 1).

To validate this prediction experimentally, we used different enzymes as topological reporters of the periplasmic and cytoplasmic sides of the membrane, namely Blam, the secreted form of β-lactamase, and Cat, respectively. Blam has been used as an alternative to the alkaline phosphatase (22) to determine the topology of different membrane proteins (27, 43); this reporter is active in the periplasm and, therefore, confers resistance to ampicillin when fused to or inserted in a region accessible to the periplasmic space (21). The cytoplasmic reporter Cat has been used in several studies to complement data obtained with either Blam or alkaline phosphatase fusions (44–46); it confers resistance to chloramphenicol when fused on the cytoplasmic side of the membrane.

Blam has been reported to be active as an in-frame insertion that can generate more useful topological information concerning a protein that is functional; on the other hand, randomly based Blam fusions enable the production of data without any assumption but can also produce false positive results (25, 21, 47). Both methods were used, limiting the analysis to fusions that conferred strong resistance to ampicillin, *i.e.* those fusions demonstrating periplasmic exposure. The location of Blam insertions was chosen based on the topological prediction (Fig. 1) and targeted to the N-terminal portion of predicted extracytoplasmic loops showing relatively low level sequence conservation.

The results obtained with Blam are presented in Table III and Fig. 2, *A* and *B*. All fusions conferring ampicillin resistance above 45 μg/ml were determined to be in-frame; the position of the preceding residue is indicated in Table III. Most fusions and insertions were detected in membrane preparations by Western blot analysis using an α-Blam antibody. Some constructs resulted in a significant amount of the low molecular weight form of immuno-reactive Blam (similar to secreted Blam), suggesting proteolysis after MntH-Blam fusions were inserted in the membrane (Phe^{38}, Gly^{49}, Val^{350}, Met^{377}, Gly^{378}, and Leu^{404} (Fig. 2*A*) and Phe^{263} and Leu^{412} (Fig. 2*B*)). In one case, a low amount of fusion protein correlated with low level Blam activity (Ala^{165}) in accordance with previous studies showing that the level of ampicillin resistance does not correlate with the level of expression of Blam fusion proteins (43, 48, 49). Hence, the two fusions that conferred lower levels of ampicillin resistance (Ala^{165} and Thr^{371}) differed significantly in their expression levels, although both were detected predominantly as Blam fusions with negligible proteolysis. This suggested that the two fusion points were located within a TMD, resulting in sub-optimal exposure of the Blam in the periplasm and, consequently, in a relatively lower level of ampicillin resistance. Three independent in-frame fusions indicated a result that is in contradiction with the prediction that placed the loop between TMDs 10 and 11 on the periplasmic *versus* the cytoplasmic side of the membrane (ambiguous location; Table III).

The three targeted Blam insertions obtained all conferred strong ampicillin resistance; two of them retained some functional activity as their expression conferred sensitivity to Fe^{2+} (supplemental data 1) and suppressed the *hflB1* (Ts) defect (Phe^{263}, Leu^{412}; Table III). They differed in their toxicity and functional activity levels, which seemed proportional to the expression levels detected using the α-Blam antibody (Fig. 2*B*). The targeted insertion Leu^{179} was hardly detectable with α-Blam, and no secreted Blam was detected either (Fig. 2*B*); however strong resistance to ampicillin (Table III) implies expression of the hybrid protein, probably at very low level. No functional activity was detected with the Leu^{179} insertion; further excision of the Blam reporter, still resulting in a GS dipeptide insertion, did not restore EcoliA activity (supplemental data 1). Insertion before the stop codon of either the Blam polypeptide (Leu^{412}) or a c-Myc tag (Leu^{412}-c-Myc; Fig. 2*C*) had similar impact, as both constructs exhibited close to wild type MntH activity (Table III). The data indicate that the (fourth) loop 6/7 (Phe^{263}) and the C terminus (Leu^{412}) are periplasmic, consistent with the topological prediction and with most Blam fusion data.

To prove the predicted cytoplasmic exposure of the loop between TMDs 10 and 11 (showing that Met^{371}, Met^{377}, and Gly^{378} in Table III represent methodological artifacts), a targeted fusion of Cat after residue 387 (Lys^{387}-Cat) was constructed; additional Cat fusion points in the loops 2/3, 6/7, and 8/9 were used as positive controls (Arg^{91}-Cat, Gly^{226}-Cat, and Leu^{324}-Cat), based on the prediction (Fig. 1), and an insertion before the stop codon was used as negative control (Leu^{412}-Cat). This C-terminal Cat insertion did not confer resistance to chloramphenicol above the background (data not shown); however, Leu^{412}-Cat was strongly expressed and toxic for cells expressing it, which limited the possible significance of the result. The addition of an N-terminal His tag was found to strongly reduce the MntH-c-Myc protein expression level (Fig. 2*C*) and diminish the toxicity of the Leu^{412}-Cat construct. Although this hybrid protein (His-Leu^{412}-Cat) was barely detectable in Western analysis of membrane preparations using an antiserum against Cat (Fig. 2*D*), it retained metal uptake activity and did not confer resistance to chloramphenicol (Table

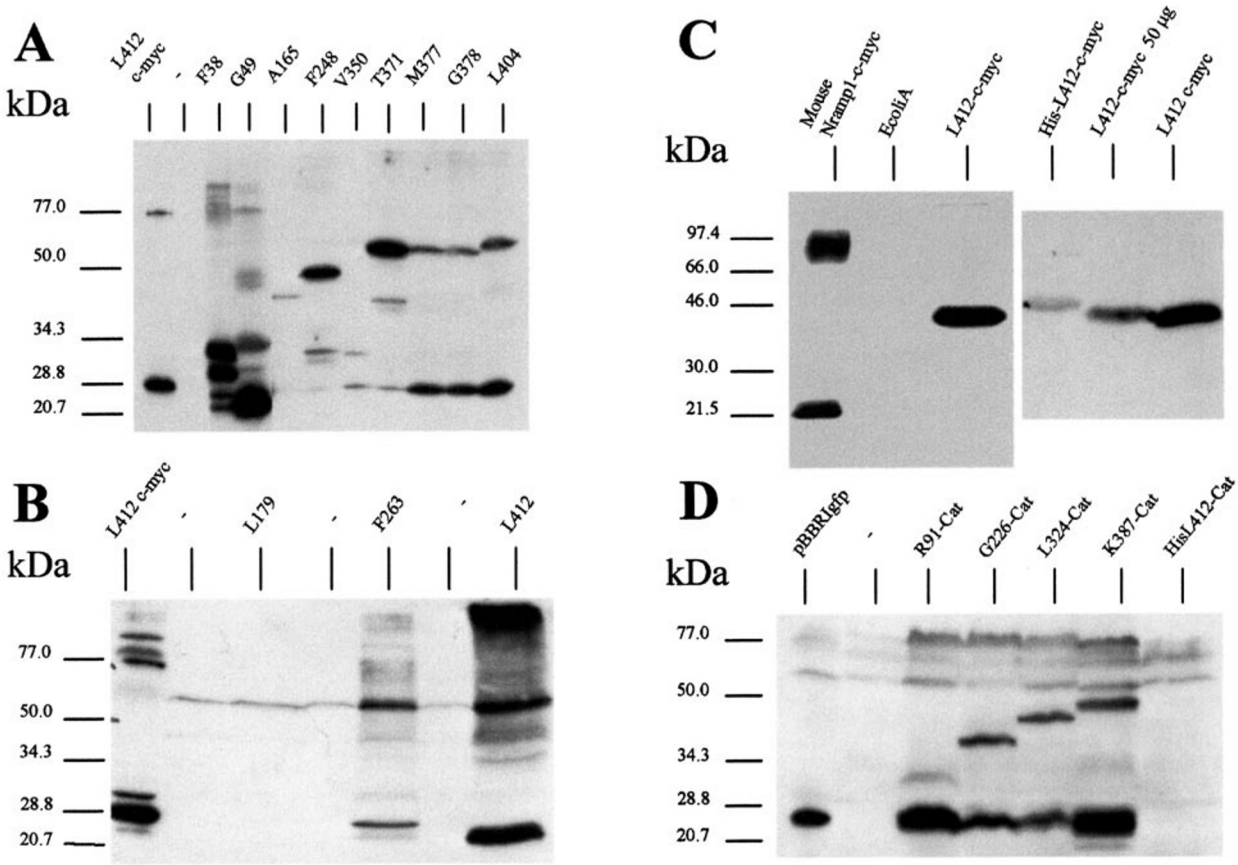

FIG. 2. **Detection of MntH mutant proteins by Western blot analysis.** *A*, *E. coli* MntH-Blam fusions. *B*, *E. coli* MntH-Blam targeted insertions. *C*, epitope-tagged MntH (Leu^{412}-c-Myc and His-Leu^{412}-c-Myc). *D*, *E. coli* MntH-Cat-targeted fusions. Equal protein amounts (120 μg per lane unless indicated otherwise) of membrane extracts prepared as described under "Experimental Procedures" were loaded for SDS-PAGE on 12% polyacrylamide gels. Single-letter amino acid symbols are used with position numbers.

TABLE IV
Analysis of Cat targeted fusions

Cml^R is chloramphenicol resistance, and NT stands for not tested.

Constructs	Cml^R	Disc assay of metal sensitivity				Suppression of *HflB1* (Ts) defect
		$FeSO_4$ (1 M)	$MnCl_2$ (1 M)	$CoCl_2$ (0.25 M)	$CdCl_2$ (0.25 M)	
	µg/ml	*mm*				
EcoliA	4	26 (± 0.5)	14 (± 0.5)	27 (± 1)	37 (± 1)	+++
Vector alone	4	14 (± 0.5)	0	10 (± 0.5)	21 (± 0.5)	−
Arg^{91}-Cat	16	NT	NT	NT	NT	NT
Gly^{226}-Cat	16	NT	NT	NT	NT	NT
Leu^{324}-Cat	12	15 (± 0.2)	0	20 (± 0.5)	28 (± 1)	+/−[a]
Lys^{387}-Cat	12	15 (± 0.2)	0	20 (± 0.5)	29 (± 1)	+/−[a]
His-Leu^{412}-Cat	4	23 (± 0.5)	0	24 (± 1)	32 (± 0.5)	+/−
His-Leu^{412}-c-Myc	4	22 (± 1)	0	31 (± 1)	32 (± 0.5)	+

[a] His-Leu^{324}-Cat, His-Lys^{387}-Cat.

IV). These results confirmed that the EcoliA C terminus is periplasmic.

Cat fusions after residues predicted to be cytoplasmic conferred accordingly strong chloramphenicol resistance (Arg^{91}-, Gly^{226}-, Leu^{324}- and Lys^{387}-Cat; Table IV). The shorter constructs conferred higher levels of resistance. Antibody reactivity against Cat was detected in membrane preparations of all of the clones expressing fusions (Fig. 2*D*). Proteolysis of these fusions was significant, in particular for Arg^{91}-Cat; this was confirmed by metabolic labeling and observation of relatively low level [^{35}S]methionine incorporation in a polypeptide of expected size and decreased protein stability after chasing with cold methionine (supplemental data 2). The deduced cytoplasmic exposure of Lys^{387} is consistent with the prediction and all other results except those of the Blam fusions Thr^{371}, Met^{377}, and Gly^{378} (Table III). These three residues precede the putative topological signal (^{384}KRVK^{387}; Fig. 1) that is believed to anchor the cytoplasmic end of TMD11 based on the "positive inside" rule (47, 48) and on other Cat fusion data obtained with EcoliA (Table IV). Expression of Leu^{324}- and Lys^{387}-Cat did not confer increased sensitivity to manganese and iron; however, residual sensitivity to the toxic metals cobalt and cadmium persisted. Expression of the Blam construct Thr^{371} (Table III) conferred similar low level sensitivity to the heavy metals cobalt and cadmium (data not shown), although in this construct, TMD10 is predicted to be inserted incorrectly in the membrane.

Disk assay of MntH-dependent metal sensitivity indicates alteration of metal transport capacity secondary to mutagenesis (Tables III and IV). However, bacterial sensitivity to heavy

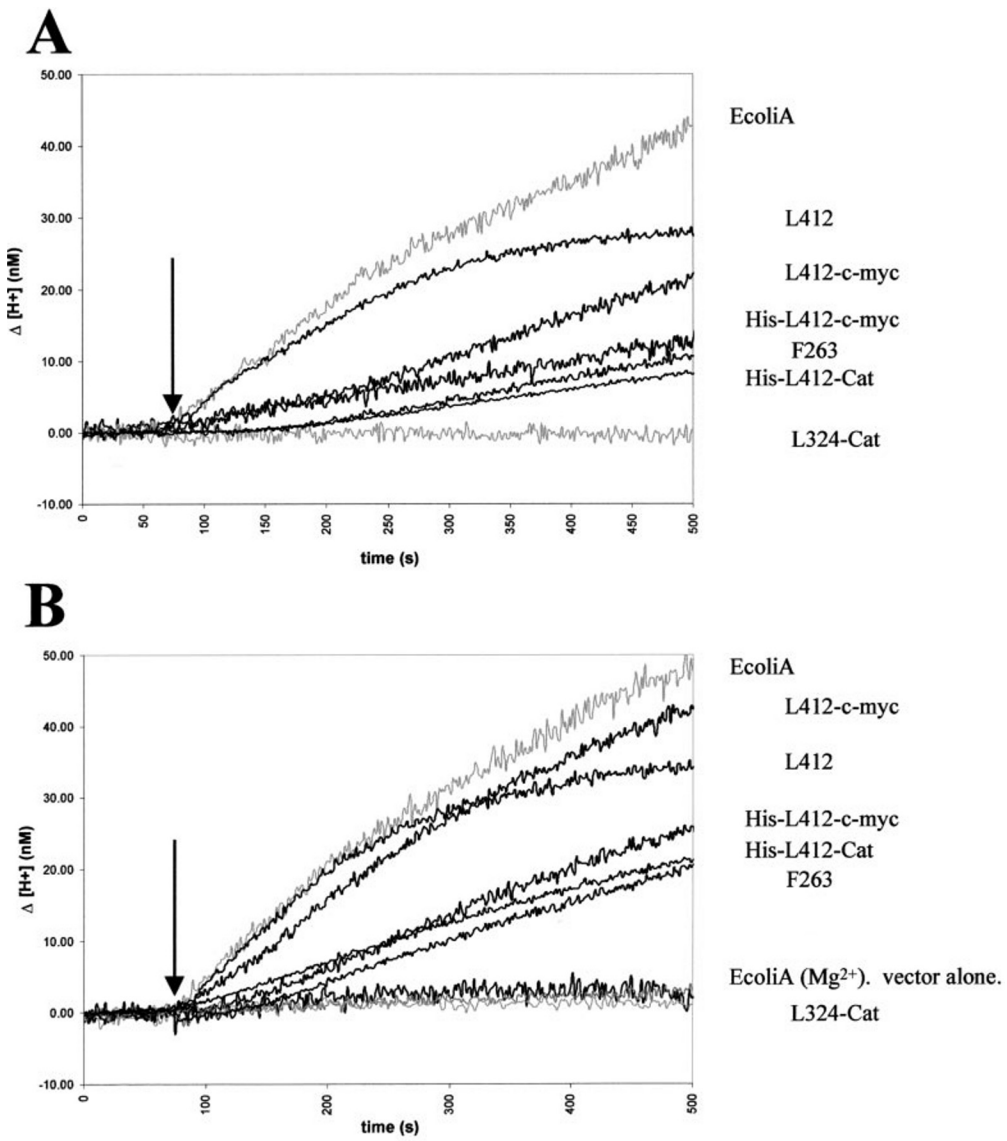

FIG. 3. **EcoliA MntH-dependent intracellular accumulation of protons in presence of cadmium (Cd^{2+}).** The intracellular accumulation of protons (*i.e.* decrease of intracellular pH) after the addition of Cd^{2+} was determined by a fluorescence assay using ratiometric green fluorescent protein as described under "Experimental Procedures." According to the calibration curve, the cadmium-dependent proton transport by wild type and mutant forms of EcoliA MntH was depicted as an increase of intracellular concentration of protons. The addition of magnesium (Mg^{2+}) to cells expressing *E. coli* MntH was used as negative control as well as the addition of 100 μM cadmium to cells without MntH (vector alone). The *arrows* indicate the addition of 10 μM $CdCl_2$ (*A*) and 100 μM $CdCl_2$ (or $MgCl_2$) (*B*). Single-letter amino acid symbols are used with position numbers.

metals such as cadmium and cobalt may be overestimated in this assay because of their inherent cytotoxicity (14). Therefore, to demonstrate the functional difference between MntH hybrid proteins (Phe^{263} and Leu^{412} (Table III) and His-Leu^{412}-Cat (Table IV)) and a truncated form of MntH (fused to Cat) that still conferred sensitivity to cadmium and cobalt (Leu^{324}-Cat, Table IV), we studied a mechanistic aspect of MntH transport. Proton-dependent transporters can use the proton electrochemical gradient to drive substrate transport against its concentration gradient. Electro-physiological measurements of eukaryotic Nramp2 activity showed that intracellular acidification accompanied divalent metal intracellular accumulation, implying proton-metal co-transport (9). To demonstrate the EcoliA MntH transport function, we examined divalent metal-dependent intracellular acidification subsequent to MntH expression using a pH-dependent ratiometric green fluorescent protein (32, 33).

The data presented in Fig. 3 show that expression of wild-type EcoliA MntH induced an intracellular acidification after the addition of Cd^{2+} but not after the addition of Mg^{2+}, indicating that a divalent metal substrate for MntH transport (1) is required for proton transport. MntH insertion mutants exhibited similar activity but with stronger dependence on the concentration of Cd^{2+} added (*e.g.* Fig. 3, *A* and *B*, Leu^{412} and Phe^{263}, Leu^{412}-c-Myc and His-Leu^{412}-c-Myc, His-Leu^{412}-c-Myc). In contrast, expression of the mutant Leu^{324}-Cat did not modulate the intracellular pH (Fig. 3), indicating the growth sensitivity to cadmium observed with this mutant is not likely due to proton-dependent transport. Expression of the construct containing the dipeptide GS inserted after Leu^{179} showed little intracellular acidification (supplemental data 1). These results demonstrate that Blam insertions within a MntH polypeptide can preserve transport function and validate the topology determination.

DISCUSSION

To our knowledge, a topological analysis demonstrating the orientation relative to the membranes of both termini and the total number of TMDs had not been previously reported for any member of Nramp family. In this work, we used functional

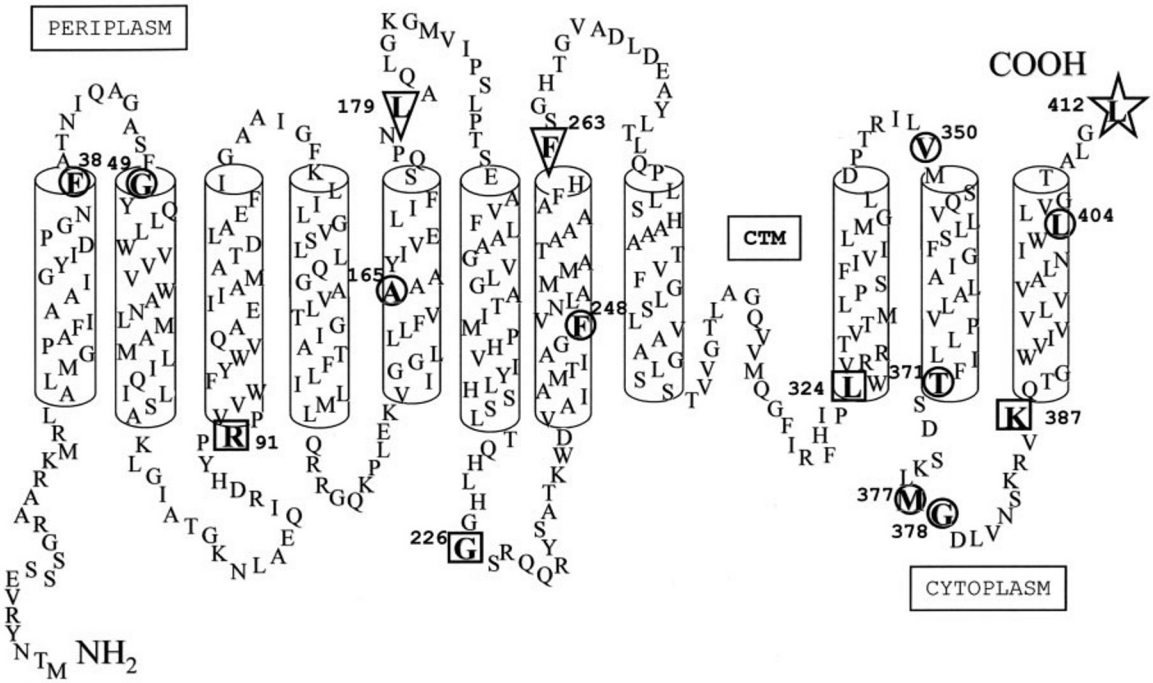

FIG. 4. **EcoliA MntH consensus transmembrane topology.** Residues upstream of Blam fusion point that were obtained by random fusion and targeted fusion of Cat are surrounded by *circles* and *squares*, respectively. Sites of targeted Blam insertions are indicated by *inverted triangles*. The last residue (Leu^{412}) is indicated by a *star* symbolizing either Blam-, c-Myc-, or Cat-targeted insertions. *Numbers* correspond to the residue positions. *CTM* indicates a predicted location of the conserved transport motif.

reporters to study the TMDs of Nramp proteins using the *E. coli* MntH A (EcoliA) ortholog as a model. The results show that EcoliA is a type III integral transmembrane protein with the N terminus cytoplasmic followed by 11 TMDs and the C terminus exposed on the periplasmic side of the membrane (Fig. 4).

The periplasmic location of the C terminus of *E. coli* MntH A was demonstrated with the C-terminal insertions of the Blam and Cat reporters that were both functional in conferring bacterial sensitivity to Fe^{2+} and Mn^{2+} and preserving divalent metal-dependent H^+-transport. Indeed, only the Blam insertion conferred resistance to ampicillin, whereas Leu^{412}-Cat did not confer chloramphenicol resistance. The intracytoplasmic location of the EcoliA N terminus was revealed by two random fusion constructs (Phe^{38} and Gly^{49}) that conferred strong resistance to ampicillin; Phe^{38} appeared predominantly in a fused form, indicating that Blam membrane insertion was due to TMD1. As the first TMD is preceded by the sequence ^{15}RKMR^{18} (that resembles the likely topological signal preceding TMD11, ^{384}KRVK^{387}), these two fusions demonstrate that the first and last hydrophobic segments of the protein constitutes TMD1. Although Pro and Gly are generally viewed as "helix-breaking" residues, their structure-based distribution in known transmembrane helices suggest a likely important structural role (50), further underscored by their conservation in Nramp TMDs, *e.g.* TMDs 1, 6, 9, and 10.

Periplasmic exposure of the predicted extra loop 6/7 was also established with the targeted Blam insertion Phe^{263} that resulted in a bi-functional hybrid protein. This result added support to that of the Blam fusion obtained within predicted TMD7 (Phe^{248}), which suggested that the carboxyl end of this transmembrane segment protruded in the periplasm. Both constructs Phe^{248} and Phe^{263} were expressed at significant levels with apparently low level of proteolysis, indicating a relative stability within the membrane. The bi-functional MntH Blam insertion (Phe^{263}) provided strong support to believe that the model presented in Fig. 4 is correct, because it preserved MntH transport of both divalent metals and protons, which is a hallmark of Nramp function. Detection of both Cd^{2+}-dependent proton transport and increased metal sensitivity (iron, cobalt, and cadmium) in cells expressing the Blam insertions Phe^{263} and Leu^{412} imply that the transmembrane topology deduced from these results describes a functional MntH A protein.

The actual number of the 11 TMDs constituting EcoliA was derived from the analysis of the 16 fusion or insertion constructs that were obtained in five of six extra loops or ends and in four of six intra loops or ends. Altogether, the Blam constructs revealed extra loops between TMDs 1 and 2, 5 and 6, 7 and 8, and 9 and 10, and the Cat constructs indicated cytoplasmic exposure of the loops 2/3, 6/7, 8/9 and 10/11. The two intra loops for which no data were produced (N terminus, intra loop 4/5) both display a significant net positive charge (+5 and +3), whereas the extra loop 3/4 has a net positive charge of +1. The amino acid composition bias of these segments thus supports their deduced localization (51).

The TMD for which no fusion was produced (TMD4) is one of the most hydrophobic in the *E. coli* MntH A protein. TMD4 is devoid of charged residues in MntH B and most MntH A proteins as well as in plant type I sequences, albeit other eukaryotic sequences and most MntH C sequences possess a conserved negative charge (Asp or Glu). Nevertheless, rat Nramp2 TMD4 was incorporated as an α-helix into micelles made of phospholipids and detergent (25), suggesting that the negative charge, when present, must be located on a side of the transmembrane helix that contributes to inter-helix contacts (50). However, a natural or an induced mutation that introduces a negatively charged residue in the N-terminal portion of TMD4 is sufficient to knock out both Nramp1 (2) and Nramp2 function (52). In any case, both the strong hydrophobicity of EcoliA TMD4 (including 14 strongly hydrophobic residues, Leu, Ile, Val, and Phe, and five residues frequently found in the lipid-exposed face of transmembrane helices, Ala and Gly) and its strong potential for internal helix packing (increased with residues Ser^{127}, Thr^{135}, and Thr^{139}) together imply, consistent

with the overall topology prediction, the existence of EcoliA TMD4.

The targeted Blam insertion in the extra loop 5/6 confirmed the result obtained with the targeted Blam fusion within TMD5 (Ala^{165}). This fusion was expressed at a low level and conferred a low level of ampicillin resistance; similarly, Blam insertion Leu^{179} was expressed at a very low level under the conditions tested and lost MntH A functional activity. Insertion of the dipeptide GS (*versus* Blam) after the residue Leu^{179} was also associated with limited EcoliA activity (both metal sensitivity and cadmium-dependent proton transport; data not shown). These results are consistent with low level expression of Leu^{179}-GS construct and indicate that the carboxyl end of TMD5 is sensitive to mutation. The sensitivity of the TMD5 carboxyl end to insertion mutagenesis would contrast with the results obtained with TMD7 in which similar mutations (Phe^{248} and Phe^{263}) resulted in rather stable polypeptides. Leu^{179} is located two residues after a Pro residue that is conserved among MntH A proteins; the sixth residue after Ala^{165} is either a polar or a charged residue, predicted to be embedded within the lipid bilayer. Hence, both the amphiphilic character of TMD5 and the presence of potential conserved structural determinants may explain the relative sensitivity of this region to insertional mutagenesis.

All the fusions and insertions that were obtained supported the consensus prediction consistently, except for three random fusions that produced an artifact (Thr^{371}, Met^{377}, and Gly^{378}). This interpretation is supported by the observation that these fusion points are localized 5–12 residues upstream of a possible topogenic signal that would anchor the TMD11 N-terminal end to the cytoplasmic side of the membrane. Therefore, all the results obtained strongly support the model derived from the consensus prediction (Figs. 1 and 4).

The 11 TMD topology (N_{in}, C_{out}) of EcoliA resembles more that of yeast proteins *versus* animal or plant homologs, which have 12 TMDs. Nevertheless, the model established in this study of the *E. coli* MntH A protein is consistent with the predictions and data that were generated studying eukaryotic homologs. The hydrophobic core that is most conserved in Nramp proteins encompasses TMDs 1–10 and implies strong structural and functional constraints to maintain both selective divalent metal transport and proton transport. The findings are consistent with the proposition that eukaryotic Nramp transporters derived from an ancestral *mntH* A gene.

Despite relatively low level sequence relationship with each other, MntH proteins from groups A and B display very similar hydropathy profiles, suggesting that MntH B proteins could adopt a transmembrane topology similar to EcoliA. Also, based on their similarity to eukaryotic Nramp, MntH C proteins should accordingly display a topology similar to the model presented, including some MntH Cβ1 proteins found in lactic bacteria predicted to contain 12 TMDs and the C terminus extracytoplasmic. In conclusion, the model established in this study will be useful for structural and functional studies of both bacterial MntH and eukaryotic Nramp transporters of divalent metals and protons.

Acknowledgments—We thank past and present lab members for their support as well as Drs. M. A. Mandrand-Berthelot, H. Ingmer, C. Dupont, and F. Shareck, who supplied reagents or shared equipment that were used in this study.

REFERENCES

1. Makui, H., Roig, E., Cole, S. T., Helmann, J. D., Gros, P., and Cellier, M. F. (2000) *Mol. Microbiol.* **35,** 1065–1078
2. Vidal, S. M., Malo, D., Vogan, K., Skamene, E., and Gros, P. (1993) *Cell* **73,** 469–485
3. Gruenheid, S., Cellier, M., Vidal, S., and Gros, P. (1995) *Genomics* **25,** 514–525
4. Belouchi, A., Cellier, M., Kwan, T., Saini, H. S., Leroux, G., and Gros, P. (1995) *Plant Mol. Biol.* **29,** 1181–1196
5. West, A. H., Clark, D. J., Martin, J., Neupert, W., Hartl, F. U., and Horwich, A. L. (1992) *J. Biol. Chem.* **267,** 24625–24633
6. Cellier, M., Prive, G., Belouchi, A., Kwan, T., Rodrigues, V., Chia, W., and Gros, P. (1995) *Proc. Natl. Acad. Sci. U. S. A.* **92,** 10089–10093
7. Cellier, M., Belouchi, A., and Gros, P. (1996) *Trends Genet.* **12,** 201–204
8. Supek, F., Supekova, L., Nelson, H., and Nelson, N. (1996) *Proc. Natl. Acad. Sci. U. S. A.* **93,** 5105–5110
9. Gunshin, H., Mackenzie, B., Berger, U. V., Gunshin, Y., Romero, M. F., Boron, W. F., Nussberger, S., Gollan, J. L., and Hediger, M. A. (1997) *Nature* **388,** 482–488
10. Forbes, J. R., and Gros, P. (2001) *Trends Microbiol.* **9,** 397–403
11. Portnoy, M. E., Liu, X. F., and Culotta, V. C. (2000) *Mol. Cell. Biol.* **20,** 7893–7902
12. Muckenthaler, M., Roy, C. N., Custodio, A. O., Minana, B., deGraaf, J., Montross, L. K., Andrews, N. C., and Hentze, M. W. (2003) *Nat. Genet.* **34,** 102–107
13. Cellier, M. F., Bergevin, I., Boyer, E., and Richer, E. (2001) *Trends Genet.* **17,** 365–370
14. Richer, E., Courville, P., Bergevin, I., and Cellier, M. (2003) *J. Mol. Evol.* **57,** 363–376
15. Que, Q., and Helmann, J. D. (2000) *Mol. Microbiol.* **35,** 1454–1468
16. Agranoff, D., Monahan, I. M., Mangan, J. A., Butcher, P. D., and Krishna, S. (1999) *J. Exp. Med.* **190,** 717–724
17. Reeve, I., Hummel, D., Nelson, N., Voss, J., and Hummell, D. (2002) *Proc. Natl. Acad. Sci. U. S. A.* **99,** 8608–8613
18. Boyer, E., Bergevin, I., Malo, D., Gros, P., and Cellier, M. F. (2002) *Infect. Immun.* **70,** 6032–6042
19. Horsburgh, M. J., Wharton, S. J., Cox, A. G., Ingham, E., Peacock, S., and Foster, S. J. (2002) *Mol. Microbiol.* **44,** 1269–1286
20. Saier, M. H. (2001) in *Microbial Transport Systems* (Winkelmann, G., ed), pp. 1–22, Wiley-VCH, Weinheim, Germany
21. van Geest, M., and Lolkema, J. S. (2000) *Microbiol. Mol. Biol. Rev.* **64,** 13–33
22. Drew, D., Sjostrand, D., Nilsson, J., Urbig, T., Chin, C. N., de Gier, J. W., and von Heijne, G. (2002) *Proc. Natl. Acad. Sci. U. S. A.* **99,** 2690–2695
23. Vidal, S. M., Pinner, E., Lepage, P., Gauthier, S., and Gros, P. (1996) *J. Immunol.* **157,** 3559–3568
24. Picard, V., Govoni, G., Jabado, N., and Gros, P. (2000) *J. Biol. Chem.* **275,** 35738–35745
25. Traxler, B., Boyd, D., and Beckwith, J. (1993) *J. Membr. Biol.* **132,** 1–11
26. Kuhn, D. E., Lafuse, W. P., and Zwilling, B. S. (2001) *J. Leukocyte Biol.* **69,** 43–49
27. Broome-Smith, J. K., and Spratt, B. G. (1986) *Gene* **49,** 341–349
28. Zhang, Y. B., and Broome-Smith, J. K. (1990) *Gene* **96,** 51–57
29. Ho, S. N., Hunt, H. D., Horton, R. M., Pullen, J. K., and Pease, L. R. (1989) *Gene* **77,** 51–59
30. Coligan, J. E., Dunn, B. M., Ploegh, H. L., Speicher, D. W., Wingfield, P. T., Bernard, A., and Payton, M. (2002) *Current Protocols in Protein Science*, Vol. 1, p. 5.2.11, John Wiley and Sons, Inc., New York
31. Ward, A., Sanderson, N. M., O'Reilly, J., Rutherford, N. G., Poolman, B., and Henderson, P. J. F. (2000) in *Membrane Transport* (Baldwin, S., ed) Oxford University Press, New York
32. Olsen, K. N., Budde, B. B., Siegumfeldt, H., Rechinger, K. B., Jakobsen, M., and Ingmer, H. (2002) *Appl. Environ. Microbiol.* **68,** 4145–4147
33. Miesenbock, G., De Angelis, D. A., and Rothman, J. E. (1998) *Nature* **394,** 192–195
34. Andersen, J. B., Sternberg, C., Poulsen, L. K., Bjorn, S. P., Givskov, M., and Molin, S. (1998) *Appl. Environ. Microbiol.* **64,** 2240–2246
35. Nilsson, J., Persson, B., and von Heijne, G. (2000) *FEBS Lett.* **486,** 267–269
36. Moller, S., Croning, M. D., and Apweiler, R. (2001) *Bioinformatics* **17,** 646–653
37. Lao, D. M., Okuno, T., and Shimizu, T. (2002) *In Silico Biol.* **2,** 485–494
38. Melen, K., Krogh, A., and von Heijne, G. (2003) *J. Mol. Biol.* **327,** 735–744
39. Jones, D. T., Taylor, W. R., and Thornton, J. M. (1994) *Biochemistry* **33,** 3038–3049
40. Krogh, A., Larsson, B., von Heijne, G., and Sonnhammer, E. L. (2001) *J. Mol. Biol.* **305,** 567–580
41. Rost, B., Fariselli, P., and Casadio, R. (1996) *Protein Sci.* **5,** 1704–1718
42. Kyte, J., and Doolittle, R. F. (1982) *J. Mol. Biol.* **157,** 105–132
43. Benoit, S., Abaibou, H., and Mandrand-Berthelot, M. A. (1998) *J. Bacteriol.* **180,** 6625–6634
44. Zelazny, A., and Bibi, E. (1996) *Biochemistry* **35,** 10872–10878
45. Adler, J., and Bibi, E. (2002) *J. Bacteriol.* **184,** 3313–3320
46. Hirata, T., Fujihira, E., Kimura-Someya, T., and Yamaguchi, A. (1998) *J. Biochem. (Tokyo)* **124,** 1206–1211
47. Ott, C. M., and Lingappa, V. R. (2002) *J. Cell Sci.* **115,** 2003–2009
48. Gunn, F. J., Tate, C. G., Sansom, C. E., and Henderson, P. J. (1995) *Mol. Microbiol.* **15,** 771–783
49. Tate, C. G., and Henderson, P. J. (1993) *J. Biol. Chem.* **268,** 26850–26857
50. Ulmschneider, M. B., and Sansom, M. S. (2001) *Biochim. Biophys. Acta* **1512,** 1–14
51. Juretic, D., Zoranic, L., and Zucic, D. (2002) *J. Chem. Inf. Comput. Sci.* **42,** 620–632
52. Fleming, M. D., Romano, M. A., Su, M. A., Garrick, L. M., Garrick, M. D., and Andrews, N. C. (1998) *Proc. Natl. Acad. Sci. U. S. A.* **95,** 1148–1153
53. Herman, C., Lecat, S., D'Ari, R., and Bouloc, P. (1995) *Mol. Microbiol.* **18,** 247–255